

See discussions, stats, and author profiles for this publication at: <https://www.researchgate.net/publication/231394927>

Plasma Polymerization of Sputtered Poly(tetrafluoroethylene)

ARTICLE *in* THE JOURNAL OF PHYSICAL CHEMISTRY · MAY 1995

Impact Factor: 2.78 · DOI: 10.1021/j100018a044

CITATIONS

53

READS

13

4 AUTHORS, INCLUDING:



José Luís Cardozo Fonseca

Universidade Federal do Rio Grande do Norte

78 PUBLICATIONS 1,216 CITATIONS

SEE PROFILE

Plasma Polymerization of Sputtered Poly(tetrafluoroethylene)

M. E. Ryan, J. L. C. Fonseca, S. Tasker, and J. P. S. Badyal*

Department of Chemistry, Science Laboratories, University of Durham, Durham DH1 3LE, U.K.

Received: December 1, 1994; In Final Form: February 15, 1995[®]

Plasma polymerization of sputtered poly(tetrafluoroethylene) (PTFE) using nonequilibrium helium, neon, argon, nitrogen, and hydrogen glow discharges has been followed by X-ray photoelectron spectroscopy (XPS), infrared spectroscopy, and UV emission spectroscopy. The chemical character of the resultant fluoropolymer deposits is found to be strongly influenced by the type of carrier gas employed.

Introduction

Nonequilibrium plasmas are useful for a variety of chemical reactions; these include the generation of atoms¹ and radicals,² isomerization,³ rearrangement,⁴ etching,⁵ and polymerization.⁶ Polymeric layers can be prepared by introducing solid-forming monomeric species into such low-temperature glow discharges. Plasma-polymerized fluoropolymer films offer many potential applications, including use as nonwetable surfaces,⁷ dielectrics,⁸ optical layers,⁹ and wear-resistant coatings.¹⁰ The most popular preparative route for synthesizing these materials is reported to be the injection of a fluoromonomer into a non-isothermal electrical discharge. Alternatively, radio-frequency (rf) sputtering of a poly(tetrafluoroethylene) (PTFE) substrate^{8,11,12} can be used, where the degree of PTFE crystallinity has been shown to exert a direct influence on the deposition rate of plasma polymer.¹¹ Such rf sputtering of PTFE is understood to evolve C₂F₄ (tetrafluoroethylene),^{11–13} which subsequently undergoes plasma polymerization in the rf sputter field.¹⁴

There has never previously been a systematic study of the influence of sputter gas on the character of the resultant plasma polymer film. In this article, the plasma polymerization of rf-sputtered PTFE is examined in the context of to what extent the chemical nature of the deposited fluoropolymer layer is influenced by the carrier gas (He, Ne, Ar, N₂, and H₂) used in the rf glow discharge. The chemical composition of the plasma phase has been followed by ultraviolet emission spectroscopy during PTFE sputtering and correlated to the chemical nature (as evaluated by X-ray photoelectron and infrared spectroscopy) of the obtained fluorocarbon deposits.

Experimental Section

High-purity helium (99.995%), neon (99.999%), argon (99.999%), nitrogen (99.993%), and hydrogen (99.999%) were used as carrier gases. Glow discharge experiments were carried out in a cylindrical glass reactor (4.5-cm diameter, 460-cm³ volume), enclosed in a Faraday cage.¹⁵ This was fitted with a gas inlet, a Pirani pressure gauge, and a 27 L min⁻¹ two-stage rotary pump attached to a liquid nitrogen cold trap. A matching network was used to inductively couple a copper coil (4-mm diameter, 9 turns, spanning 8–15 cm from the gas inlet) wound around the reactor to a 13.56-MHz rf source. All joints were grease free. Gas and leak flow rates were calculated assuming ideal gas behavior.¹⁶

A typical experimental run comprised initially scrubbing the reactor with detergent, rinsing with isopropyl alcohol, and oven drying, followed by a high-power (50-W) air plasma treatment for 40 min. This latter step was done in the presence of glass substrates but in the absence of any polymer film. Then the

entire inner walls of the glass reactor were lined with fresh PTFE film (Mupor Ltd.), and the reactor was pumped down to a base pressure of 1.5×10^{-3} Torr with a leak rate better than 4.0×10^{-3} cm³ min⁻¹. Subsequently, the carrier gas of interest was introduced into the reaction chamber at 2×10^{-1} Torr pressure and a flow rate (F_V) of 1.62×10^{-2} cm³ s⁻¹ (i.e., at least 99.6% of F_V is the feed gas). After allowing 5 min for purging, the glow discharge was ignited at 50 W for 20 min. Upon termination of deposition, the radio-frequency source was switched off, and the carrier gas was allowed to purge the system for 5 min and then vented to atmosphere.

A Kratos ES200 spectrometer was used for X-ray photoelectron spectroscopy (XPS) analysis. This was operated in the fixed analyzer transmission (FAT) mode, at a pass energy of 65 eV and an electron take-off angle of 30° from the substrate normal. Magnesium K_α X-rays were used as the photoexcitation source. Instrument performance was calibrated with respect to the gold 4f_{7/2} peak at 83.8 eV with a full width at half-maximum (FWHM) of 1.2 eV. No radiation damage was observed during the typical time scale involved in these experiments. An IBM PC computer was used for data accumulation and component peak analysis (assuming linear background subtraction and Gaussian fits with fixed FWHM).¹⁷ All binding energies are referenced to the hydrocarbon component.¹⁸ Instrumentally determined sensitivity factors for unit stoichiometry were taken as C(1s):O(1s):F(1s):N(1s):Si(2p) equaling 1.00:0.46:0.33:0.37:1.31.

A FTIR Mattson Polaris instrument was used for transmission infrared analysis of rf plasma-sputtered fluorocarbon layers deposited onto pressed potassium bromide (KBr) disks. A reference infrared spectrum of PTFE substrate was obtained by using a variable angle attenuated total reflection (ATR) cell fitted with a KRS-5 crystal; an incident beam angle of 45° resulted in 14 internal reflections. Typically, 100 scans were acquired at a resolution of 4 cm⁻¹.

A home-built UV emission spectrometer based upon a Czerny–Turner-type monochromator was used for plasma glow analysis. A computer was used to rotate the grating via a stepping motor and also to accumulate the counts from the photomultiplier tube detector. This instrument could scan continuously from 180 to 500 nm at 0.5-nm resolution.

Results

(a) X-ray Photoelectron Spectroscopy. Clean PTFE displays a main C(1s) peak at 291.2 eV and a weak Mg K_{α3,4} satellite shifted by approximately 9 eV toward lower binding energy, Figure 1a. For each type of glow discharge treatment investigated, there was negligible variation in the C(1s) envelope across the rf coils, which suggests a homogeneous chemical composition. This observation is consistent with the whole of the reactor being lined with PTFE and, therefore, being able to

* To whom correspondence should be addressed.

[®] Abstract published in *Advance ACS Abstracts*, April 1, 1995.

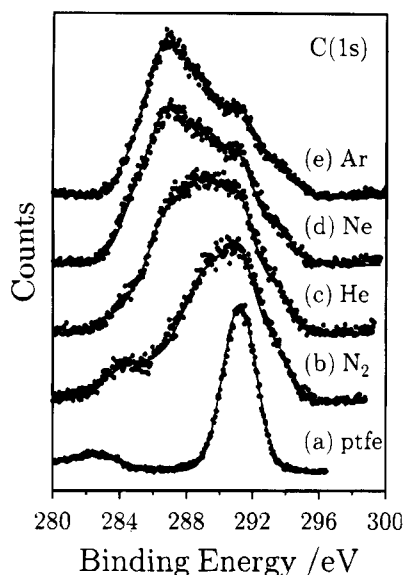


Figure 1. C(1s) XPS spectra of (a) clean PTFE, (b) nitrogen-sputter-deposited perfluoro polymer, (c) helium-sputter-deposited perfluoro polymer, (d) neon-sputter-deposited perfluoro polymer, and (e) argon-sputter-deposited perfluoro polymer.

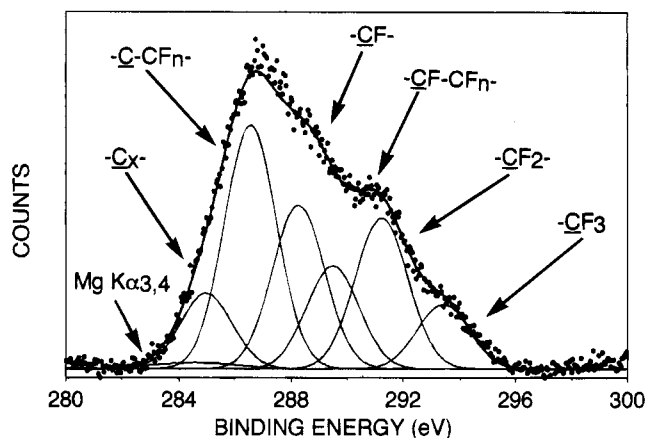


Figure 2. Typical C(1s) XPS peak fit (Argon glow discharge, 50 W).

provide a uniform source of polymerizable species. The absence of any Si(2p) signal from the underlying glass slide substrate was taken as being indicative of complete coverage by the plasma polymer. A small amount of oxygen- and nitrogen-containing functionalities was detected by XPS, the most likely origin of these being reaction between trapped free-radical centers at the surface and the laboratory atmosphere during transport of the deposited layer from the glow discharge apparatus to the XPS spectrometer¹⁹ (contamination within the bulk of the deposited fluoro polymer layer can be ruled out since oxygenated carbon functionalities were absent in the transmission infrared analysis of these films). The C(1s) XPS spectra of each coating were fitted with six Mg K $\alpha_{1,2}$ components having equal FWHM corresponding to CF₃ (293.6 eV), CF₂ (291.2 eV), CFCF_n (289.5 eV), CF (288.3 eV), CCF_n (286.6 eV), and C_x (284.6 eV) environments,²⁰ Figure 2. Additional Mg K $\alpha_{3,4}$ satellites²¹ shifted by approximately 9 eV toward lower binding energy (with a different fixed FWHM) were also taken into consideration. Table 1 summarizes the relative proportions of fluorinated carbon centers measured for each glow discharge treatment. Surprisingly, no fluoropolymer deposition was observed for the hydrogen carrier gas experiments. Fluoropolymer deposits resulting from the noble gas plasmas displayed a gradual loss in fluorine content with increasing atomic mass of the carrier gas, while nitrogen plasma sputtering of PTFE produced the greatest CF₂ component.

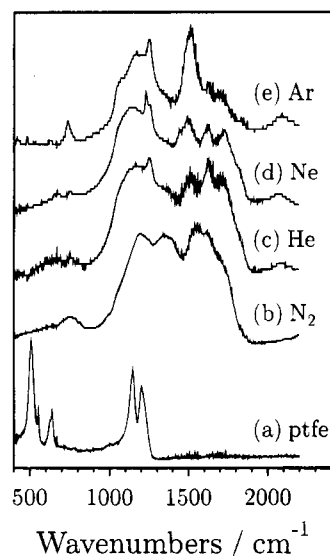


Figure 3. FTIR absorbance spectra of (a) clean PTFE, (b) nitrogen-sputter-deposited perfluoro polymer, (c) helium-sputter-deposited perfluoro polymer, (d) neon-sputter-deposited perfluoro polymer, and (e) argon-sputter-deposited perfluoro polymer.

TABLE 1: Summary of C(1s) XPS Peak Fits (NB [Total C] = [C] + [CCF_n], and [Total CF] = [CF] + [CFCF_n])

		100%				100%			
	F:C	total C	total CF	CF ₂	CF ₃	% C	% F	% N	% O
PTFE	2.00	0.0	0.0	100.0	0.0	33.7	66.3	0.0	0.0
N ₂	1.21	14.6	37.5	34.9	13.1	40.1	48.6	8.7	2.5
He	1.02	25.6	39.9	25.4	9.2	45.3	46.0	3.1	5.6
Ne	0.82	38.8	33.4	20.2	7.5	50.7	41.3	1.0	7.0
Ar	0.78	39.7	33.2	18.9	8.0	52.0	40.4	0.9	6.8

(b) Infrared Spectroscopy. Absorbances in the ATR-FTIR spectrum of clean PTFE can be assigned as follows:²² 514 cm⁻¹ (CF₂ wagging), 556 cm⁻¹ (CF₂ rocking), 640 cm⁻¹ (CF₂ rocking), 1152 cm⁻¹ (asymmetric C-F stretch), 1208 cm⁻¹ (symmetric C-F stretch).

Infrared absorption bands in the sputter-deposited fluoro polymer layers were assigned as follows: 740 cm⁻¹ (CF₃ stretching deformation²³ and/or symmetric CF₂ vibration which becomes active due to distortion of (CF₂)_n chains²⁴), 1000–1400 cm⁻¹ (C-F stretching^{25–27}), 1515 cm⁻¹ (absorbances in this region have been previously observed for plasma polymers prepared from perfluorobenzene²⁸), 1626 cm⁻¹ (CF=C< stretch in a cross-linked environment^{25,29}), 1730 cm⁻¹ (CF=CF stretch^{25,26,29,30}), and 2077 cm⁻¹ (CF=C=CF stretching—fluorine substitution causes a shift to higher vibrational frequencies away from the usual 2000–1900-cm⁻¹ region^{25,29}). On moving from nitrogen to helium to neon to argon, the 1515-cm⁻¹ absorbance rises in intensity at the expense of the 1626- and 1730-cm⁻¹ features; this is consistent with a greater number of cross-linked/aromatic environments.

(c) UV Emission Spectroscopy. Common methods used for identifying and monitoring the intermediates within fluorocarbon plasmas include mass spectrometry and emission spectroscopy. Mass spectrometry can be used to sample ions and radicals or analyze stable end products in the effluent.^{31–33} Emission spectroscopy is useful for identifying excited intermediates within the plasma phase, although the determination of absolute concentrations requires knowledge of the relative amounts of ground- and excited-state species.³⁴ Since the optical diagnostic tool is external to the reactive plasma chamber, this makes it a nonintrusive technique, enabling the direct observation of short-lived species.³⁵ Previous conclusions obtained by effluent mass spectrometry for fluorocarbon discharges tie in with the appropriate optical emission spectra.³⁵ For instance, CF₂ species

are believed to play an important role in fluorocarbon plasmas,^{32,36–40} where the rate of plasma polymerization has been shown to correlate with the CF_2 radical concentration in the glow discharge.^{41–43}

Assignment of emission spectra from fluorocarbon plasmas can be complicated.⁴⁴ A number of bands in the 197–420-nm UV region are reported to be characteristic of CF, CF_2 , and CF_3 radical species;^{44,45} these provide a basis for identification of emission bands obtained in the present study. UV emission spectra were acquired for excited glow discharges of helium, neon, argon, and nitrogen gas in the absence and presence of PTFE, Figure 4. Two UV band systems are observed for CF: these being ($\text{A}_2\Sigma^+ - \text{X}^2\Pi$) and ($\text{B}^2\Delta - \text{X}^2\Pi$) transitions in the 220–295-nm^{48,56} and 197–220-nm^{46,56} ranges, respectively. The $\text{CF}_2(^1\text{B}_1 - ^1\text{A}_1)$ band system at 240–325 nm⁴⁵ has been previously noted for C_2F_4 , perfluoropropene (C_3F_6), and perfluorobutene (C_4F_8) plasmas.^{39,44,45,49–52} There is some overlap here with the $\text{CF}(\text{A}^2\Sigma^+ - \text{X}^2\Pi)$ transition between 220 and 295 nm. UV emission features for CF_3 radicals are reported to have been observed by Suto *et al.*^{57–59} in the 180–300-nm region; however, a theoretical analysis by Larrieu *et al.*⁶⁰ raises some ambiguities concerning this assignment of CF_3 bands. In fact, the main UV emission features for CF_3 radicals occur in the 450–750-nm region,⁵⁷ while atomic F lines appear in the 680–720-nm region;^{61–64} unfortunately for both of these species, there is no overlap with the scan range available in the present study. The disappearance of any lines from the pure gas glow discharge during PTFE sputter plasma polymerization can be explained in terms of the absorption of these lines by sputtered fluorocarbon species.

In the case of helium plasma treatment of PTFE, all peaks between 320 and 500 nm can be assigned to helium, Figure 4a. Forty-four lines in the $\text{CF}_2(^1\text{B}_1 - ^1\text{A}_1)$ band system are evident between 240 and 320 nm (many more than for neon), and only one CF band is evident at 202.3 nm ($\text{B}^2\Delta - \text{X}^2\Pi$ transition). Furthermore, 14 of the lines which appeared in the pure helium glow discharge are absent during sputter deposition, Figure 4a.

The UV emission peaks measured during neon glow discharge sputtering of PTFE spectrum can be assigned to neon, CF_2 or CF transitions, Figure 4b. All of the bands in the 280–500 nm range are characteristic of a clean neon plasma. The intense feature at 240–280 nm can be resolved into 30 lines of the $\text{CF}_2(^1\text{B}_1 - ^1\text{A}_1)$ band system. The lines at 229.6 and 223.2 nm are $\text{CF}(\text{A}^2\Sigma^+ - \text{X}^2\Pi)$ transitions, and those at 207.7 and 202.4 nm are $\text{CF}(\text{B}^2\Delta - \text{X}^2\Pi)$ transitions. Twelve of the UV emission bands seen for the pure neon glow discharge were found to disappear during rf sputtering of PTFE.

Apart from one intense line at 253.3 nm from the $\text{CF}_2(^1\text{B}_1 - ^1\text{A}_1)$ band system, all of the UV emission bands identified during argon plasma treatment of PTFE originate from the argon glow discharge, Figure 4c. Three characteristic bands of the pure argon plasma at 388.0, 357.4, and 336.9 nm were also absent during glow discharge sputtering of PTFE.

Most of the peaks observed during nitrogen glow discharge sputtering of PTFE can be assigned to those characteristic of pure nitrogen plasmas.⁶⁵ Figure 4d. Additional band heads are present at 394.0, 370.8, 297.6, 296.1, and 295.7 nm; the last three of these peaks fall in the $\text{CF}_2(^1\text{B}_1 - ^1\text{A}_1)$ region, although exact assignment is difficult. It is of interest to note that the overall absolute UV spectral intensity was greatest for the pure nitrogen glow discharge; this can be explained in terms of each nitrogen molecule effectively dissociating to form two excitable nitrogen atoms.

Discussion

Decomposition of PTFE during glow discharge sputtering results mainly in the evolution of tetrafluoroethylene. These

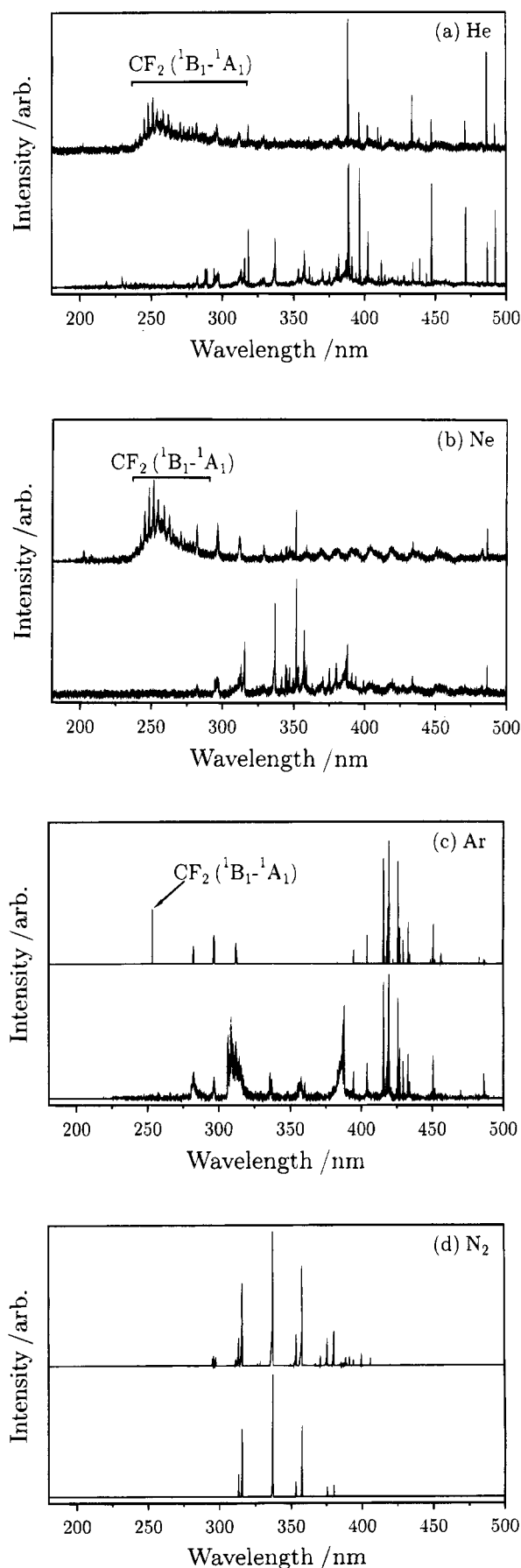


Figure 4. UV emission spectra of glow discharge in the absence (lower) and presence (upper) of PTFE film in the 180–500-nm region: (a) He, (b) Ne, (c) Ar, and (d) N_2 .

species undergo plasma polymerization in the vicinity of the electromagnetic sputter field.^{11,13,66} High-deposition rates occur

when a carrier gas (such as argon) is used during rf sputtering of PTFE,⁶⁷ this behavior may be attributed to greater momentum transfer (substrate etching) by the heavier argon species.⁶⁸ Modification of the PTFE substrate itself is also reported to take place during exposure to inert gas, nitrogen, and hydrogen plasmas.^{69,70}

XPS analysis has shown that the fluorine content drops on moving from helium to neon to argon glow discharges; this appears to be a direct manifestation of momentum transfer phenomena.^{68,71} The CF₂ wagging and rocking vibrations in the infrared fingerprint region of PTFE are not evident in the plasma polymer spectra; this can be taken as being indicative of a highly cross-linked fluorocarbon network. Since the CF₂-(¹B₁-¹A₁) UV emission band system is evident for all of the noble gas sputter plasma polymerization experiments, it is instructive to compare the number of lines present in the CF₂-(¹B₁-¹A₁) band system for each gas, although no conclusions can be made from the absolute line intensities because these will depend upon the type of noble gas atom used. On moving from helium to neon to argon, it is found that during glow discharge sputtering of PTFE there is a decrease in the number of lines contained in the CF₂-(¹B₁-¹A₁) band system, which can be attributed to absorption of the emitted CF₂-(¹B₁-¹A₁) band system lines by unsaturated fluorocarbon species, resulting in their effective absence. Overall, a direct correlation exists between the level of defluorination in the sputtered coating as measured by XPS, the FTIR absorbance strength of the carbon-rich/cross-linked/aromatic species, and the observed attenuation in the number of lines contained in the CF₂-(¹B₁-¹A₁) band system due to photoabsorption by unsaturated fluorocarbon moieties. The nitrogen glow discharge UV emission results are anomalous due to the very intense lines of nitrogen itself, which effectively masked out any fluorocarbon features.

The stark contrast in deposition behavior between hydrogen and helium carrier gas experiments is slightly puzzling at first glance, since both gases are very light, yet no plasma polymer was generated in the case of hydrogen. There are two possible explanations for this paradox: either the sputter rate is very low for a hydrogen glow discharge, or the evolved species may not readily succumb to plasma polymerization but prefer to form stable byproducts, e.g., HF and CH₄. Surface modification of PTFE by a hydrogen plasma is reported to result in defluorination of the polymer substrate via HF elimination⁶⁵ (i.e., hydrogen atom exchange with the PTFE backbone⁶⁹). Indeed, very low concentrations of carbon-containing moieties are evolved during the exposure of a fluoropolymer surface to a hydrogen glow discharge, whereas all noble gases (including helium) eject a variety of fluorocarbon species into the plasma phase.⁶⁵

Fluoropolymer films deposited from nitrogen glow discharge sputtering of PTFE appear to yield the highest F:C ratio. Since atomic nitrogen (atomic mass = 14) does not differ significantly from neon (atomic mass = 20), this anomalous behavior by the nitrogen plasma can be attributed to either a greater density of sputtering moieties (dissociation of each nitrogen molecule in the glow discharge will generate two nitrogen atoms) or some type of chemical interaction between excited nitrogen species and the PTFE substrate (e.g., the formation of excimers).

Conclusions

Nonequilibrium glow discharge treatment of PTFE results in the simultaneous sputtering of the substrate accompanied by the plasma polymerization of ablated fluorocarbon species. In the case of noble gases, the extent of fragmentation and defluorination can be accounted for in terms of a simple momentum transfer model, whereas additional chemical factors may be in play in the case of hydrogen and nitrogen glow discharges.

Acknowledgment. M.E.R. thanks Mupor Ltd. for financial support during the course of this work.

References and Notes

- (1) Wagner, H. G.; Wolfrum, J. *Angew. Chem.* **1971**, *83*, 561.
- (2) Suhr, H. *Plasma Chem. Plasma Process.* **1983**, *3*, 1.
- (3) Suhr, H.; Schucher, U. *Synthesis* **1970**, 431.
- (4) Wells, R. K.; Drummond, I. W.; Robinson, K. S.; Street, F. J.; Badyal, J. P. S. *J. Chem. Soc., Chem. Commun.* **1993**, 6, 549.
- (5) Egitto, F. D.; Vukanovic, V.; Taylor, G. N. In *Plasma Deposition, Treatment, and Etching of Polymers*; d'Agostino, R., Ed.; Academic: San Diego, 1990; Chapter 5.
- (6) Biederman, H.; Osada, Y. *Adv. Polym. Sci.* **1990**, *95*, 59.
- (7) Yasuda, H. *Plasma Polymerization*; Academic: London, 1985.
- (8) Pratt, I. H.; Lausman, T. C. *Thin Solid Films* **1972**, *10*, 151.
- (9) Martinu, L.; Biederman, H. *Vacuum* **1986**, *36*, 477.
- (10) Sugimoto, I.; Miyake, S. *J. Appl. Phys.* **1991**, *70*, 2618.
- (11) Morrison, D. T.; Robertson, T. *Thin Solid Films* **1973**, *15*, 87.
- (12) Jackson, N. F.; Harrop, P. J. Br. Patent 1226946, 1971.
- (13) Mathias, E.; Muller, C. H. *J. Phys. Chem.* **1967**, *71*, 2673.
- (14) Tibbitt, J. M.; Shen, M.; Bell, A. T. *Thin Solid Films* **1975**, *29*, L43.
- (15) Shard, A. G.; Munro, H. S.; Badyal, J. P. S. *Polym. Commun.* **1991**, *32*, 152.
- (16) Ehrlich, C. D.; Basford, J. A. *J. Vac. Sci. Technol.* **1992**, *A10*, 1.
- (17) Evans, J. F.; Gibson, J. H.; Moulder, J. F.; Hammond, J. S.; Goretzki, H. *Fresenius Z. Anal. Chem.* **1984**, *319*, 841.
- (18) Johansson, G.; Hedman, J.; Berndtsson, A.; Klasson, M.; Nilsson, R. *J. Electron Spectrosc.* **1973**, *2*, 295.
- (19) Sharma, A. K.; Yasuda, H. *J. Appl. Polym. Sci.* **1989**, *38*, 741.
- (20) Clark, D. T.; Feast, W. J.; Ritchie, I.; Musgrave, W. K. R.; Modena, M.; Ragazzini, M. *J. Polym. Sci., Polym. Chem. Ed.* **1974**, *1*, 1049.
- (21) Wagner, C. D.; Riggs, W. M.; Davis, L. E.; Moulder, J. F.; Muilenberg, G. E. *Handbook of X-Ray Photoelectron Spectroscopy*; Perkin-Elmer: New York, 1978; p 13.
- (22) Starkweather, H. W.; Ferguson, R. C.; Chane, D. B.; Minor, J. M. *Macromolecules* **1985**, *18*, 1684.
- (23) Haque, Y.; Ratner, B. D. *J. Polym. Sci., Polym. Phys. Ed.* **1988**, *27*, 3965.
- (24) Giegengack, H.; Hinze, D. *Phys. Stat. Solid.* **1971**, *A8*, 513.
- (25) Bellamy, L. J. *The Infra-Red Spectra of Complex Molecules*; Wiley: New York, 1975; Vol. 1.
- (26) Buzzard, P. D.; Soong, D. S.; Bell, A. T. *J. Appl. Polym. Sci.* **1982**, *27*, 3965.
- (27) Sugimoto, I. *Macromolecules* **1991**, *24*, 1480.
- (28) Inagaki, N.; Kibayashi, N.; Matsushima, M. *J. Membrane Sci.* **1988**, *38*, 85.
- (29) Silverstein, R. M.; Bassler, G. C.; Morrill, T. C. *Spectrometric Identification of Organic Compounds*; Wiley: New York, 1981.
- (30) Dias, A. J.; McCarthy, T. J. *Macromolecules* **1985**, *18*, 1826.
- (31) Studniarz, S. A. In *Ion-Molecule Reactions*; Franklin, J. L., Ed.; Plenum: New York, 1972; Vol. 2, pp 647-671.
- (32) Vasile, M. J.; Smolinsky, G. *J. Phys. Chem.* **1977**, *81*, 2605.
- (33) Smolinsky, G.; Vasile, M. J. *Eur. Polym. J.* **1979**, *15*, 87.
- (34) Miller, T. A. In *Annual Review of Physical Chemistry*; Rabinovich, B. S., Ed.; Annual Review: Los Angeles, 1976; Vol. 27, pp 127-152.
- (35) Millard, M. M.; Kay, E. *J. Electrochem. Soc.* **1982**, *129*, 160.
- (36) Powell, F. X.; Lide, D. R. *J. Chem. Phys.* **1966**, *45*, 1067.
- (37) Bass, A. M.; Mann, D. E. *J. Chem. Phys.* **1962**, *36*, 3501.
- (38) Dyke, J. M.; Golob, L.; Johnathan, N.; Morris, A.; Okuda, M. *J. Chem. Soc., Faraday Trans. 2* **1974**, *70*, 1828.
- (39) King, D. S.; Schenck, P. K.; Stephenson, J. C. *J. Mol. Spectrosc.* **1979**, *78*, 1.
- (40) Smith, O. E.; Jacox, M. E.; Milligan, D. E. *J. Mol. Spectrosc.* **1976**, *60*, 381.
- (41) Kay, E.; Coburn, J. W.; Kruppa, G. *LeVide* **1976**, *183*, 89.
- (42) Kay, E.; Dilks, A.; Coburn, J. In *Topics in Current Chemistry*; Veprek, S.; Venugopalan, M., Eds.; Springer Verlag: Berlin, 1980; pp 1-54.
- (43) Dilks, A.; Kay, E. In *Plasma Polymerization*; Shen, M.; Bell, A. T., Eds.; ACS Symposium Series; American Chemical Society: Washington, DC, 1979; pp 195-218.
- (44) Koda, S. *Chem. Phys. Lett.* **1978**, *55*, 353.
- (45) Venkateswarlu, P. *Phys. Rev.* **1950**, *77*, 676.
- (46) Andrews, E. B.; Barrow, R. F. *Proc. R. Phys. Soc., London* **1951**, *A64*, 481.
- (47) Thrush, B. A.; Zwolenik, J. J. *J. Chem. Soc., Trans. Faraday Soc.* **1963**, *59*, 582.
- (48) Porter, T. L.; Mann, D. E.; Acquista, N. *J. Mol. Spectrosc.* **1965**, *16*, 228.
- (49) Mathews, C. W. *Can. J. Phys.* **1967**, *45*, 2355.
- (50) Marsigny, L.; Ferran, J.; Lebreton, J.; Legrange, R. *C. R. Acad. Sci., Paris, Ser. C* **1968**, *266*, 9, 507.
- (51) Gilbert, R.; Thoret, A. *J. Phys. Chem.* **1976**, *80*, 1017.

- (52) Trung, Q.; Durocher, G.; Sauvageau, P.; Dorfy, C. *Chem. Phys. Lett.* **1977**, *47*, 404.
- (53) Staemmler, V. *Theor. Chim. Acta* **1974**, *35*, 309.
- (54) Sam, C. L.; Yardley, J. T. *Chem. Phys. Lett.* **1979**, *61*, 509.
- (55) Tiee, J. J.; Wampler, F. B.; Rice, W. W. *Chem. Phys. Lett.* **1979**, *68*, 403.
- (56) Pearse, R. W. B.; Gayson, A. G. *The Identification of Molecular Spectra*; Chapman and Hall: London, 1976.
- (57) Suto, M.; Washida, N. *J. Chem. Phys.* **1983**, *78*, 1007.
- (58) Suto, M.; Washida, N. *J. Chem. Phys.* **1983**, *78*, 1012.
- (59) Suto, M.; Washida, N.; Akimoto, H.; Nakamura, M. *J. Chem. Phys.* **1983**, *78*, 1019.
- (60) Larrieu, C.; Chaillet, M.; Dargelos, A. *J. Chem. Phys.* **1992**, *96*, 3732.
- (61) Harshbarger, W. R.; Porter, R. A.; Miller, T. A.; Norton, P. *Appl. Spectrosc.* **1977**, *31*, 201.
- (62) Mogab, C. J.; Adams, A. C.; Flamm, D. L. *J. Appl. Phys.* **1978**, *49*, 3796.
- (63) Frieser, R. G.; Nogay, J. *Appl. Spectrosc.* **1980**, *34*, 31.
- (64) Donnelly, V. M.; Flamm, D. L. *Abstract 123*; Extended Abstracts; The Electrochemical Society: St. Louis, 1980; p 323.
- (65) Gallaher, T. W.; De Vore, T. C.; Carter, R. O.; Anderson, C. *Appl. Spectrosc.* **1980**, *34*, 408.
- (66) Coburn, J. W.; Eckstein, E. W.; Kay, E. J. *Vac. Sci. Technol.* **1975**, *12*, 151.
- (67) Holland, L.; Biederman, H.; Ojha, S. M. *Thin Solid Films* **1976**, *35*, L19.
- (68) Thornton, J. A. In *Deposition Technologies for Films and Coatings*; Bunshah, R. F., Ed.; Noyes: Englewood Cliffs: NJ, 1982; Chapter 2.
- (69) Clark, D. T.; Hutton, D. R. *J. Polym. Sci., Polym. Chem. Ed.* **1987**, *25*, 2643.
- (70) Yasuda, H.; Marsh, H. C.; Brandt, S.; Reilley, C. N. *J. Polym. Sci., Polym. Chem. Ed.* **1977**, *15*, 991.
- (71) Yamada, Y.; Kurobe, T. *Jpn. J. Appl. Phys.* **1993**, *32*, 5090.

JP943187N